Rubbed Polyimide Surface Studied by Sum-Frequency Vibrational Spectroscopy

Doseok Kim*

Department of Physics, Sogang University, Seoul, 121-742 Korea

Masahito Oh-e† and Y. R. Shen

Department of Physics, University of California at Berkeley, Berkeley, California 94720

Received January 17, 2001; Revised Manuscript Received July 31, 2001

ABSTRACT: Surface-specific sum-frequency vibrational spectroscopy was used to study the structure of a rubbed polyimide surface. The spectra showed that the polymer backbones were well aligned by rubbing along the rubbing direction, and the imide cores were inclined toward the surface plane with a broad distribution. Quantitative analysis yields an approximate orientational distribution function for the aligned imide cores and the backbones.

Introduction

Mechanical rubbing of polymer-coated substrates is commonly used to homogeneously align liquid crystal (LC) films in the LC display industry.[1] Presumably, rubbing aligns the surface polymer chains, which in turn aligns the LC monolayer adsorbed on the polymer surface. The latter then determines the LC orientation and alignment throughout the bulk film through correlation of LC molecules.[2] Detailed understanding of the alignment mechanism would help the design of LC display cells. Thus many studies of the problem using various techniques such as infrared spectroscopy,[3−5] optical retardation,[1,6] ellipsometry,[7] scanning force microscopy,[8−10] X-ray scattering,[11] and X-ray spectroscopy[12−15] have been reported in the literature. Recently infrared-visible sum-frequency vibrational spectroscopy has been demonstrated to be an effective probe for polymer surfaces.[16−18] It has the advantage of being surface-specific and sensitive to the surface monolayer. Application of the technique to a rubbed surface of poly(vinyl alcohol) (PVA) was able to yield quantitative information about the orientation and alignment of PVA chains at the surface.[17] In the LC display industry, however, polyimide (PI) is the preferred polymeric material for LC alignment. It is therefore important to carry out a similar study on PI. We present here the results of such a study.

There exist already many reports on investigation of rubbed PI.[3−15] In particular, surface second harmonic generation (SHG) which is a special case of sum-frequency generation (SFG) has been used to study side-chain PI.[19,20] In these experiments, however, SHG is mainly generated from the side chains of the polymer, and does not yield information about rubbing-induced alignment of the main chains. Yet it is the latter that is responsible for the surface-induced homogeneous alignment of LC films. With SFG spectroscopy, we were able to measure the anisotropy induced by rubbing in the vibrational spectrum of CO groups associated with the imide rings of PI at the surface. The results allowed us to deduce an approximate orientational distribution of the imide rings, and hence of the PI main chains, at the rubbed surface.

Experimental Section

The polymide used in our experiment was poly(*n*-alkylpyromelitic imide) [$-N-(CO)_2-C_6H_2-(CO)_2-N-(CH_2)_n$], with $n = 6$ (P6). Its chemical structure is shown in Figure 1a. The polymer film was prepared by spin-coating the polyamic precursor onto a fused silica plate and letting the solvent evaporate for 1 h at 60 °C. Subsequently, the sample was baked at 200 °C for 2 h and cured at 300 °C for 5 h. The film thickness determined from atomic force microscopic measurement was about 40 nm. The PI film was then rubbed with velvet cloth. The rubbing strength used for the sample was at the saturation level, such that further rubbing would not enhance the observed anisotropy in the SFG spectra.

The experimental setup for SFG has been described elsewhere.[21] In brief, a pulsed Nd:YAG laser system was used to generate a visible beam at 532 nm and a tunable IR beam around 5.9 μm, both having a 15 ps pulse width and a 20 Hz repetition rate. The two beams coming in from the air side overlapped at the sample surface, and the SFG output was detected in the reflection direction.

Theory

Theoretically, the surface SFG signal intensity generated by the input fields with intensities $I_1(\omega_{vis})$ and $I_2(\omega_{ir})$ can be expressed by the following equation[17]

$$I(\omega_{SF}) = \frac{8\pi^3\omega_{SF}^2 \sec^2\beta_{SF}}{c^3}|\chi_{eff}^{(2)}|^2 I_1(\omega_{vis})I_2(\omega_{ir}) \quad (1)$$

where β_{SF} is the angle of the sum-frequency output with respect to the surface normal. The effective nonlinearity $\chi_{eff}^{(2)}$ takes the form of

$$\chi_{eff}^{(2)} = [\hat{e}(\omega_{SF})\cdot\overleftrightarrow{L}(\omega_{SF})]\cdot\overleftrightarrow{\chi}^{(2)}: [\hat{e}(\omega_{vis})\cdot\overleftrightarrow{L}(\omega_{vis})][\hat{e}(\omega_{ir})\cdot\overleftrightarrow{L}(\omega_{ir})] \quad (2)$$

with $\hat{e}(\omega)$ being the unit polarization vector and $\overleftrightarrow{L}(\omega)$ the tensorial Fresnel factor at frequency ω.[21] The nonlinear susceptibility $\overleftrightarrow{\chi}^{(2)}$ can be written as

$$\overleftrightarrow{\chi}^{(2)} = \overleftrightarrow{\chi}_{NR}^{(2)} + N_s\int\overleftrightarrow{\alpha}^{(2)}(\Omega)f(\Omega)d\Omega \quad (3)$$

† Current Address: Hitachi, Ltd., Displays, 3300 Hayano, Mobara-shi, Chiba-ken, 297-8622 Japan.

10.1021/ma0100908 CCC: $20.00
Published on Web 11/22/2001

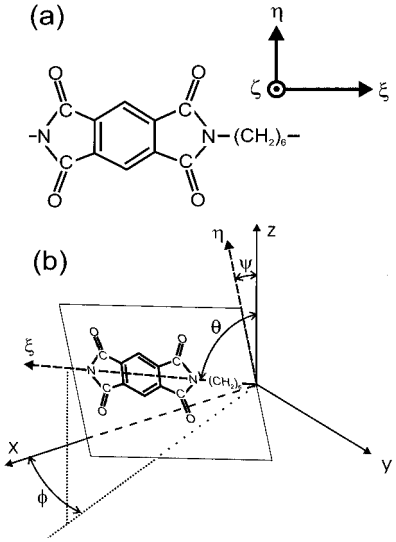

Figure 1. (a) Chemical structure of P6 polyimide, shown with a set of molecular coordinates (ξ, η, ζ). (b) Relation between the laboratory coordinates (x, y, z) and the molecular coordinates (ξ, η, ζ) of an imide group. x is along the rubbing direction and z the surface normal. The imide ring lies in the shadowed plane ($\xi - \eta$), and ψ is the angle between the imide ring plane and the z-axis. The ζ-axis is normal to the imide ring plane.

where the resonant molecular hyperpolarizability $\overleftrightarrow{\alpha}^{(2)}$ can be written as

$$\overleftrightarrow{\alpha}^{(2)}(\omega_{ir}, \Omega) = \sum_q \frac{\overleftrightarrow{a}_q}{(\omega_{ir} - \omega_q) + i\Gamma_q} \tag{4}$$

such that

$$\overleftrightarrow{\chi}^{(2)}(\omega_{ir}) = \overleftrightarrow{\chi}^{(2)}_{NR} + \sum_q \frac{\overleftrightarrow{A}_q}{(\omega_{ir} - \omega_q) + i\Gamma_q}$$

with

$$\overleftrightarrow{A}_q = N_s \int \overleftrightarrow{a}_q(\Omega) f(\Omega) d\Omega \tag{5}$$

Here $\chi^{(2)}_{NR}$ denotes the nonresonant contribution, $\overleftrightarrow{a}_q$, ω_q, and Γ_q are the strength, resonant frequency, and damping constant of the qth resonant mode, and Ω represents a set of orientational angles (θ, ϕ, ψ) defined in Figure 1b. It is known that the vibrationally resonant SFG can be considered as a combined process of a resonant infrared excitation step followed by an anti-Stokes Raman step. The quantity a_q in eq 4 can be written in terms of the product of the infrared dipole derivative and the Raman polarizability tensor of the qth vibrational mode, $\partial\mu/Q_q$ and $\partial\alpha^{(1)}/Q_q$, respectively

$$(a_q)_{lmn} = -\frac{1}{2\omega_q} \frac{\partial \alpha^{(1)}_{lm}}{\partial Q_q} \frac{\partial \mu_n}{\partial Q_q} \tag{6}$$

where Q_q denotes the normal mode coordinates, and the sub-indices (l, m, n) refer to the molecular coordinates (ξ, η, ζ) described in Figure 1a.

Results and Discussion

In the experiment, we have measured the SFG spectra of rubbed PI in the C=O stretch vibration region. Shown in Figure 2 are the representative spectra taken at three different angles (γ = 0, 90, and 180°)

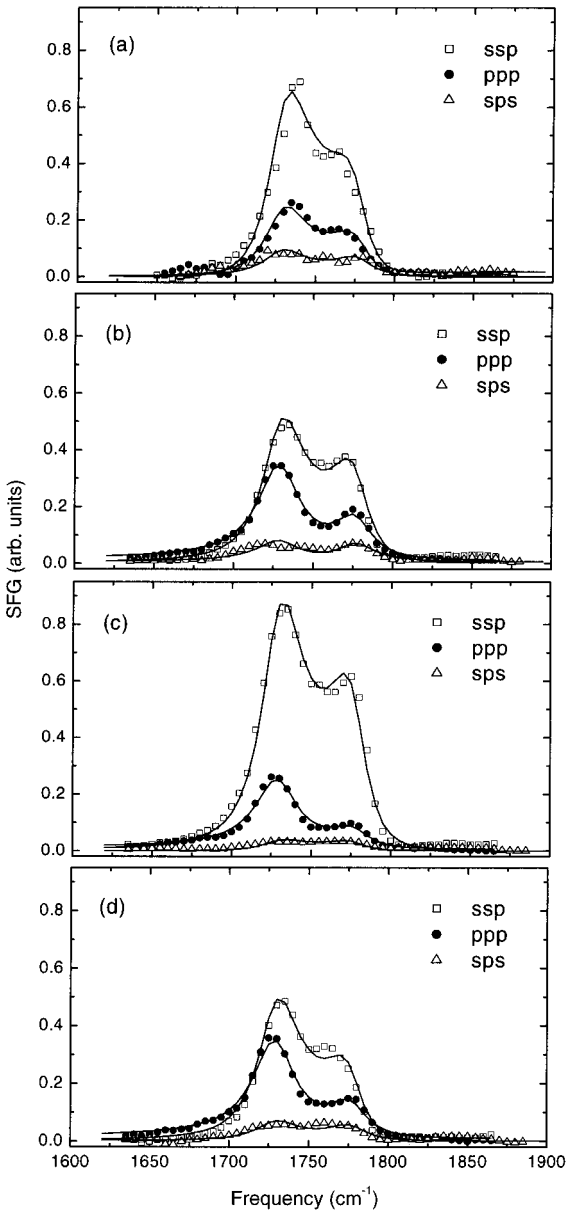

Figure 2. SFG spectra of (a) unrubbed and rubbed polyimide films (b–d). Beam propagation direction is (b) parallel, (c) 90°, and (d) antiparallel to the rubbing direction. Solid lines in the figure are fits to the experimental data following eq 5.

between the incidence plane and the rubbing direction with three input/output polarization combinations: SSP (denoting S-polarized SF output, S-polarized visible input, and P-polarized infrared input, respectively), SPS, and PPP. All the spectra can be fitted by eq 5 with two resonant modes, one at 1729 cm^{-1} with a half-width of 16 cm^{-1}, and the other at 1777 cm^{-1} with a half-width of 14 cm^{-1}. They can be assigned to the antisymmetric (a) and symmetric (s) stretch vibrational modes, respectively, for two coupled CO moieties associated with each imide ring.[22]

These spectra originated mainly from the air/rubbed PI interface. To check for the possibility of SFG coming from the polymer bulk and PI/substrate interface, the sample was briefly etched in an NaOH solution.[18] The initial film was thin enough such that infrared beam can reach the back polymer/substrate interface (for possible generation of SFG at the back surface) without much attenuation, and the bulk of the polymer was

nearly intact by etching as confirmed by the UV−visible absorption measurement. Yet the SFG spectra diminished drastically after the treatment, indicating that contributions from the PI/substrate interface or the polymer bulk are negligible. This agrees well with the previous experiments which showed the SFG signal of the polymer was mainly from the air/polymer interface.[16,23]

From surface to bulk, the polymer has its structural units changed from a more ordered orientational distribution to a random distribution. The CO bonds not exposed to air are expected to form quadrupole pairs with CO bonds of neighboring molecular units. Then as quadrupoles, they contribute very weakly to SFG. For SFG in reflection, total quadrupole contribution comes effectively only from CO in a layer of 20 nm below the polymer/air interface. Most of this layer has the bulk structure and a significantly weaker average quadrupole contribution per CO pair than that in the surface-bulk transition layer because of the random CO orientation in the bulk structure. From the above presumptions, one can easily show that the quadrupole contribution is negligible compared with the dipole contribution from the CO monolayer protruding out of the surface as long as the average distance between CO in a quadrupole pair is smaller than that between two CO attached to the same imide ring.[24]

Following these considerations, inspection of the spectra in Figure 2 readily provides a qualitative picture for the rubbing-induced alignment of the imide cores, and hence the PI backbones. First, the SSP spectrum at $\gamma = 90°$ is significantly stronger than the one at $\gamma = 0$ or 180°, indicating that the imide cores, and hence the PI backbones, are more or less along the rubbing direction. Second, the near forward−backward symmetry suggests that the polymer backbones lie nearly flat on the surface. A very weak forward−backward asymmetry can be observed in the PPP spectra, corresponding to a slight upward tilt of the chains along the rubbing direction at the surface. Thus rubbing appears to have induced, on average, a PI orientation well along the rubbing direction at the surface. The degree of anisotropy in the spectra is a measure of how broad a distribution the chain orientation has around its mean.

In the more quantitative analysis, we deduced first the values for the nonvanishing elements of $(A_q)_{ijk}$ for each mode (q = a and s) from the spectral data, and then from eq 5, find an approximate orientational distribution $f(\Omega)$. For a rubbed surface with the rubbing direction along x (and the surface normal along z), the C_{1v} symmetry allows 10 independent nonvanishing elements of $(A_q)_{ijk}$ for each mode. They are[17]

$$(A_q)_{xxz}, (A_q)_{yyz}, (A_q)_{zzz}, (A_q)_{xzx} = (A_q)_{zxx}, (A_q)_{yzy} = (A_q)_{zyy}, (A_q)_{xxx}, (A_q)_{yyx}, (A_q)_{zzx}, (A_q)_{xzz} = (A_q)_{zxz}, (A_q)_{xyy} = (A_q)_{yxy} \quad (7)$$

The last five elements would vanish if the forward−backward symmetry along x also holds. We can obtain the values of the nonvanishing $(A_q)_{ijk}$ from the experimentally determined values of $A_{q,\mathrm{eff}}(\gamma, \mathrm{P})$ for different sample orientations γ and input/output polarization combinations P using eq 2, which remains valid if $\chi^{(2)}$ is replaced by A_q. Equation 2 yields the following equations.

$$A_{q,\mathrm{eff}}(\gamma, \mathrm{SSP}) = \sin\beta_{\mathrm{ir}} L_{yy}(\omega_{\mathrm{SF}}) L_{yy}(\omega_{\mathrm{vis}}) L_{zz}(\omega_{\mathrm{ir}}) ((A_q)_{yyz} \cos^2\gamma + (A_q)_{xxz} \sin^2\gamma) + [(((A_q)_{xxx} - (A_q)_{xyy} - (A_q)_{yxy}) \sin^2\gamma \cos\gamma + (A_q)_{yyx} \cos^3\gamma) \times \cos\beta_{\mathrm{ir}} L_{yy}(\omega_{\mathrm{SF}}) L_{yy}(\omega_{\mathrm{vis}}) L_{xx}(\omega_{\mathrm{ir}})] \quad (8)$$

$$A_{q,\mathrm{eff}}(\gamma, \mathrm{SPS}) = \sin\beta_{\mathrm{vis}} L_{yy}(\omega_{\mathrm{SF}}) L_{zz}(\omega_{\mathrm{vis}}) L_{yy}(\omega_{\mathrm{ir}}) ((A_q)_{yzy} \cos^2\gamma + (A_q)_{xzx} \sin^2\gamma) + [(((A_q)_{xxx} - (A_q)_{yyx} - (A_q)_{xyy}) \sin^2\gamma \cos\gamma + (A_q)_{xyy} \cos^3\gamma) \times \cos\beta_{\mathrm{vis}} L_{yy}(\omega_{\mathrm{SF}}) L_{xx}(\omega_{\mathrm{vis}}) L_{yy}(\omega_{\mathrm{ir}})]$$

$$A_{q,\mathrm{eff}}(\gamma, \mathrm{PPP}) = -\cos\beta_{\mathrm{SF}} \cos\beta_{\mathrm{vis}} \sin\beta_{\mathrm{ir}} \times L_{xx}(\omega_{\mathrm{SF}}) L_{xx}(\omega_{\mathrm{vis}}) L_{zz}(\omega_{\mathrm{ir}}) \times ((A_q)_{xxz} \cos^2\gamma + (A_q)_{yyz} \sin^2\gamma) + \sin\beta_{\mathrm{SF}} \sin\beta_{\mathrm{vis}} \sin\beta_{\mathrm{ir}} \times L_{zz}(\omega_{\mathrm{SF}}) L_{zz}(\omega_{\mathrm{vis}}) L_{zz}(\omega_{\mathrm{ir}}) (A_q)_{zzz} - \cos\beta_{\mathrm{SF}} \sin\beta_{\mathrm{vis}} \cos\beta_{\mathrm{ir}} L_{xx}(\omega_{\mathrm{SF}}) L_{zz}(\omega_{\mathrm{vis}}) L_{xx}(\omega_{\mathrm{ir}}) \times ((A_q)_{xzx} \cos^2\gamma + (A_q)_{yzy} \sin^2\gamma) + \sin\beta_{\mathrm{SF}} \cos\beta_{\mathrm{vis}} \cos\beta_{\mathrm{ir}} L_{zz}(\omega_{\mathrm{SF}}) L_{xx}(\omega_{\mathrm{vis}}) L_{xx}(\omega_{\mathrm{ir}}) \times ((A_q)_{zxx} \cos^2\gamma + (A_q)_{zyy} \sin^2\gamma) + [(\sin\beta_{\mathrm{SF}} \cos\beta_{\mathrm{vis}} \sin\beta_{\mathrm{ir}} (L_{zz}(\omega_{\mathrm{SF}}) L_{xx}(\omega_{\mathrm{vis}}) L_{zz}(\omega_{\mathrm{ir}}) (A_q)_{zxz} - \cos\beta_{\mathrm{SF}} \sin\beta_{\mathrm{vis}} \sin\beta_{\mathrm{ir}} L_{xx}(\omega_{\mathrm{SF}}) L_{zz}(\omega_{\mathrm{vis}}) L_{zz}(\omega_{\mathrm{ir}})) (A_q)_{xxz} + \sin\beta_{\mathrm{SF}} \sin\beta_{\mathrm{vis}} \cos\beta_{\mathrm{ir}} L_{zz}(\omega_{\mathrm{SF}}) L_{zz}(\omega_{\mathrm{vis}}) L_{xx}(\omega_{\mathrm{ir}})) (A_q)_{zzx}) \cos\gamma - ((A_q)_{xxx} \cos^3\gamma + ((A_q)_{yyx} + (A_q)_{yxy} + (A_q)_{xyy}) \sin^2\gamma \cos\gamma) \times \cos\beta_{\mathrm{SF}} \cos\beta_{\mathrm{vis}} \cos\beta_{\mathrm{ir}} L_{xx}(\omega_{\mathrm{SF}}) L_{xx}(\omega_{\mathrm{vis}}) L_{xx}(\omega_{\mathrm{ir}})]$$

In the above equations, the terms inside the square brackets are the terms allowed only when forward−backward asymmetry is broken, and therefore can be treated as a perturbation in the analysis. Moreover, since $\beta_{\mathrm{SF}} = 46.1°$ is almost the same as $\beta_{\mathrm{vis}} = 45°$ in our experimental geometry, the local field factors in front of the third and fourth terms of $A_{q,\mathrm{eff}}(\gamma, \mathrm{PPP})$ are nearly the same. This together with the fact that the visible input beam is nonresonant (thus $(A_q)_{xzx} = (A_q)_{zxx}$) makes these two terms of $A_{q,\mathrm{eff}}(\gamma, \mathrm{PPP})$ practically cancel each other. In our analytical procedure, we first deduced the values of $A_{q,\mathrm{eff}}(\gamma, \mathrm{P})$ for different γ and the polarizations by fitting the measured SFG spectra using eq 5, knowing that the peak positions and widths do not change with γ and the polarizations. We then used eq 8 to fit the data points of $A_{q,\mathrm{eff}}(\gamma, \mathrm{P})$ assuming the forward−backward symmetry (neglecting the terms inside the square brackets), and deduce the values of the top five nonvanishing $(A_q)_{ijk}$ in eq 7. Finally, we included in eq 8 the correction terms from the other five $(A_q)_{ijk}$ in eq 7 (terms inside the square brackets) to take into account the weak forward−backward asymmetry. The values of these five $(A_q)_{ijk}$ that are expected to be small were then obtained from a perturbation calculation to match the observed forward−backward asymmetry. In Figure 3, we show the data points of $A_{q,\mathrm{eff}}(\gamma, \mathrm{P})$ deduced from the measured spectra and the fit of the data points for the antisymmetric mode. Listed in Table 1 are the values of all nonvanishiing $(A_q)_{ijk}$ deduced from such an analysis. In the calculation, we used the refractive indices of $n = 1.7$ for PI and $n = 1.46$ for fused quartz to estimate the values for the Fresnel factors L in eq 8 and assumed that L was dispersionless. Because the PI film thickness is only ~40 nm, its effect on L is less than 5% compared to the case without the PI film.

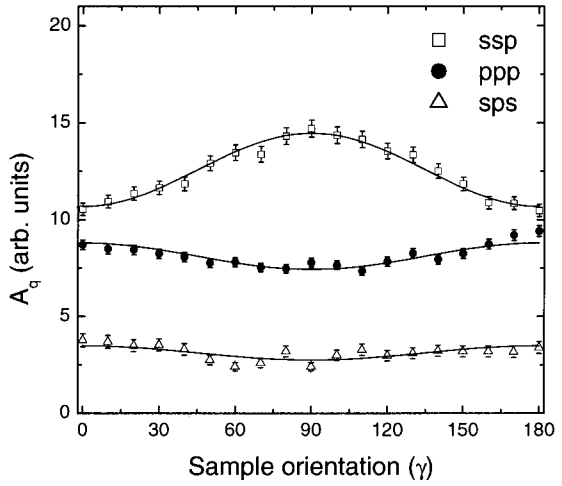

Figure 3. Angular dependence of the SFG peak strength A_a at 1729 cm^{-1}. The lines are fits to the data using the first five $(A_q)_{ijk}$ values in Table 1.

Table 1. Measured and Calculated Nonvanishing Tensor Elements A_{ijk} for *a* and s Modes of C=O[a]

	a-mode		*s*-mode	
	measured	calculated	measured	calculated
A_{xxz}	48 ± 2	47.8	−34 ± 2.5	−31.8
A_{yyz}	36 ± 2	36.7	−25 ± 2.5	−25.1
A_{zzz}	40 ± 5	40.1	−27 ± 4	−27.0
$A_{xzx} = A_{zxx}$	10 ± 1.5	8.4	−8 ± 1	−6.1
$A_{yzy} = A_{zyy}$	15 ± 2	17.2	−13 ± 2	−12.4
A_{xxx}	1.7 ± 0.4	1.7	∼0	0.7
A_{yyx}	−0.5 ± 0.5	0	∼0	0
A_{zzx}	0.5 ± 0.4	0.7	∼0	0.3
$A_{xyy} = A_{yxy}$	∼0	0	∼0	0
$A_{xzz} = A_{zxz}$	∼0	−0.4	∼0	−0.1

[a]The nonlinearities in the first five rows are the ones expected from the C_{2v} symmetry, and the ones below are expected when the forward−backward symmetry is broken.

Knowing the values of $(A_q)_{ijk}$, we can now use eq 5 to find an approximate $f(\Omega)$ for the (ξ, η, ζ) molecular frame. For this purpose, we need to know $\vec{\vec{a}}_q(\Omega)$ in terms of θ, ϕ, and ψ. The first step is to find the nonvanishing elements of $\vec{\vec{a}}_q$ in the molecular coordinates. Consider an imide core with four CO groups described in Figure 4. The CO−CO coupling across the central benzene ring is expected to be weak so that we can treat the four CO's as two independent groups. The two CO's in each group are coupled, giving rise to the antisymmetric and symmetric stretch vibration modes. Altogether, there are four possible stretch modes for the four CO groups shown in Figure 4. We now recall from earlier discussion that the imide rings are expected to lie along the surface and only the CO bonds protruding out of the surface (say, the upward pointing bonds in Figure 4) contribute significantly to surface SFG. Symmetry consideration of such a case then requires that the dominating elements of $\vec{\vec{a}}_q$ are $((a_q)_{\xi\xi\eta}$ and $(a_q)_{\eta\eta\eta}$ for q = s and a, which are only associated with modes a and c in Figure 4. For modes b and d, the nonvanishing elements are $(a_q)_{\xi\eta\xi} = (a_q)_{\eta\xi\xi}$, but because the CO bonds are nearly parallel to the η axis, they are relatively small and can be neglected. Consequently, for a PI molecular unit with orientation specified by $\Omega = (\theta, \phi, \psi)$ (Figure 1b), we have the following relations between tensorial elements of $\vec{\vec{a}}_q$ in the lab coordinates and in the molecular coordinates

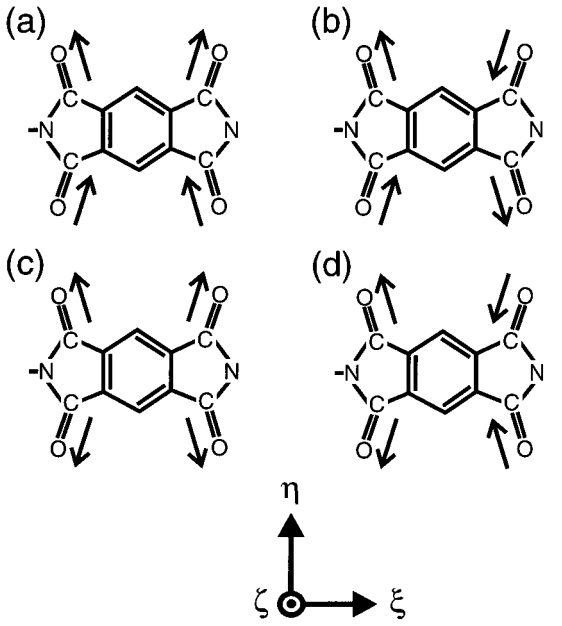

Figure 4. Possible normal modes of CO stretch vibrations for monomer unit: (a, b) antisymmetric stretches; (c, d) symmetric stretches.

$$(a_q)_{xxz} = 2(a_q)_{\xi\xi\eta}\langle(\hat{\xi}\cdot\hat{x})(\hat{\xi}\cdot\hat{x})(\hat{\eta}\cdot\hat{z})\rangle + 2(a_q)_{\eta\eta\eta}\langle(\hat{\eta}\cdot\hat{x})(\hat{\eta}\cdot\hat{x})(\hat{\eta}\cdot\hat{z})\rangle$$
$$= -2(a_q)_{\xi\xi\eta}\langle\sin^3\theta\rangle\langle\cos^2\phi\rangle\langle\cos\psi\rangle - 2(a_q)_{\eta\eta\eta}(\langle\sin\theta\rangle\langle\sin^2\phi\rangle\langle\sin^2\psi\cos\psi\rangle + \langle\sin\theta\cos^2\theta\rangle\langle\cos^2\phi\rangle\langle\cos^3\psi\rangle)$$

$$(a_q)_{yyz} = -2(a_q)_{\xi\xi\eta}\langle\sin^3\theta\rangle\langle\sin^2\phi\rangle\langle\cos\psi\rangle - 2(a_q)_{\eta\eta\eta}(\langle\sin\theta\rangle\langle\cos^2\phi\rangle\langle\sin^2\psi\cos\psi\rangle + \langle\sin\theta\cos^2\theta\rangle\langle\sin^2\phi\rangle\langle\cos^3\psi\rangle)$$

$$(a_q)_{zzz} = -2(a_q)_{\xi\xi\eta}\langle\sin\theta\cos^2\theta\rangle\langle\cos\psi\rangle - 2(a_q)_{\eta\eta\eta}\langle\sin^3\theta\rangle\langle\cos^3\psi\rangle$$

$$(a_q)_{xzx} = 2(a_q)_{\xi\xi\eta}\langle\sin\theta\cos^2\theta\rangle\langle\cos^2\phi\rangle\langle\cos\psi\rangle - 2(a_q)_{\eta\eta\eta}(\langle\sin\theta\rangle\langle\sin^2\phi\rangle\langle\sin^2\psi\cos\psi\rangle + \langle\sin\theta\cos^2\theta\rangle\langle\cos^2\phi\rangle\langle\cos^3\psi\rangle)$$

$$(a_q)_{yzy} = 2(a_q)_{\xi\xi\eta}\langle\sin\theta\cos^2\theta\rangle\langle\sin^2\phi\rangle\langle\cos\psi\rangle - 2(a_q)_{\eta\eta\eta}(\langle\sin\theta\rangle\langle\cos^2\phi\rangle\langle\sin^2\psi\cos\psi\rangle + \langle\sin\theta\cos^2\theta\rangle\langle\sin^2\phi\rangle\langle\cos^3\psi\rangle) \quad (9)$$

and five other similar equations for the five other $(a_q)_{ijk}$ elements whose orientational average would vanish with forward−backward symmetry. We use these expressions for $(a_q)_{ijk}$ in eq 5 and assume that $f(\Omega)$ can be approximated by a Gaussian form

$$f(\Omega) = C\exp\left[-\frac{(\theta-\theta_0)^2}{2\sigma_\theta^2} - \frac{(\phi-\phi_0)^2}{2\sigma_\phi^2} - \frac{(\psi-\psi_0)^2}{2\sigma_\psi^2}\right] \quad (10)$$

where C is a normalization constant and θ_0, ϕ_0, ψ_0, σ_θ, σ_ϕ, and σ_ψ are parameters to be determined. We limit the ranges of θ and ϕ between 0 and 180° and ψ between 0° and 90°. For the C_{1v} symmetry of a rubbed surface, $\phi_0 = 0°$. We then have altogether a set of 20

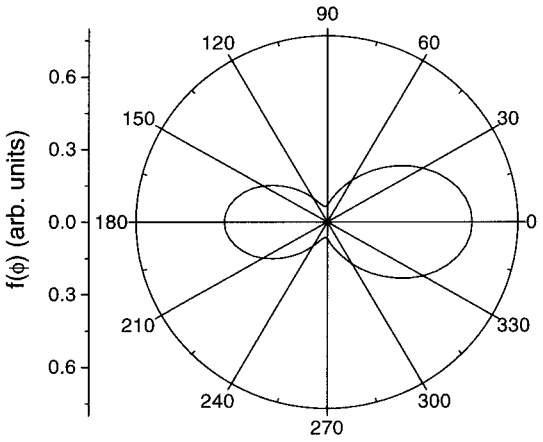

Figure 5. Azimuthal orientational distribution function of the polyimide backbone obtained from eq 10 after integration over θ and ψ. 0° is along the rubbing direction.

equations to determine only five parameters θ_0, ψ_0, σ_θ, σ_ϕ, and σ_ψ, plus the ratio of $(a_q)_{\eta\eta\eta}/(a_q)_{\xi\xi\eta}$. A unique solution from the equations would indicate that the experimental data are reliable and the theoretical model is reasonable.

In our calculations for the rubbed PI, we first assumed forward−backward symmetry, and therefore, $\theta_0 = 90°$. Using the deduced values of the first five $(A_q)_{ijk}$ elements (q = a and s) in Table 1 in their corresponding equations, we obtained $(a_a)_{\eta\eta\eta}/(a_a)_{\xi\xi\eta} = 1.13 \pm 0.05$, $(a_s)_{\eta\eta\eta}/(a_s)_{\xi\xi\eta} = 1.25 \pm 0.06$, $\sigma_\theta = 9° \pm 2°$, $\sigma_\phi = 39° \pm 5°$, and $\psi_0 = 65° \pm 25°$ with σ_ψ varying from ∼12° at $\psi_0 = 40°$ to ∼76° at $\psi_0 = 90°$. The values of ψ_0 and σ_ψ suggest that the imide core plane is inclined toward the surface plane with a rather broad distribution. We could use a step-function distribution instead of the Gaussian distribution to describe the orientational distribution of the imide core planes. The result is similar. For example, we found that $f(\psi)$ = constant for $90° > \psi > 8°$, and $f(\psi) = 0$ otherwise, can fit the experimental result equally well. This is qualitatively the same as the Gaussian distribution with $\psi_0 = 90°$ and $\sigma_\psi = 76°$.

We next considered forward−backward asymmetry and included the values of the previously neglected $(A_q)_{ijk}$ elements in the calculation. We found $\theta_0 = 88° \pm 1°$, with the other parameters hardly changed. To show consistency of the result, we used the deduced $f(\Omega)$ to reevaluate $(A_q)_{ijk}$. The calculated values of $(A_q)_{ijk}$, also listed in Table 1 are indeed close to those deduced from the measurement.

The deduced orientational distribution function $f(\Omega)$ shows that on a rubbed PI surface, the PI backbones are preferentially aligned along the rubbing direction with a somewhat broad distribution in ϕ ($\sigma_\phi = 39°$). The backbones lie nearly flat on the surface with only a small average upward tilt (∼2°) along the rubbing direction. This tilt angle or the forward−backward asymmetry is responsible for the observed bulk pretilt angle in the liquid crystal films sandwiched between rubbed PI-coated substrates. It is smaller than the tilt angle (∼10°) of the liquid crystal monolayer adsorbed on top of the rubbed polyimide film, but larger than the bulk pretilt angle.[2] Presented in Figure 5 is a plot of the azimuthal orientational distribution of the backbones obtained from integration of $f(\Omega)$ over θ and ψ. As compared with the azimuthal distribution of the LC monolayer on rubbed PI (the same P6 polymer),[2] the asymmetry of PI is clearly weaker.

Our result on the rubbed PI surface is in good agreement with those obtained with near-edge X-ray absorption fine structure (NEXAFS) method.[12−15] In the latter studies, azimuthal orientation of the backbones along the rubbing direction and the small upward tilt of the polymer chain were also observed with polyimdes of different chemical structures. The imide core plane was found to lie flat on the surface,[13−15] but it could also have a broad distribution as we have deduced from our SFG result (e.g., $\psi_0 = 90°$ and $\sigma_\psi = 76°$). In conclusion, we have shown that sum-frequency vibrational spectroscopy is useful as an analytical tool to determine the anisotropic surface structure of a polymer. We have found that mechanical rubbing can effectively induce an alignment of the surface polyimide chains along the rubbing direction with a slight upward tilt. The imide core planes, however, are inclined toward the surface with a rather broad distribution. The aligned polyimide surface is apparently the reason for the observed alignment of the liquid crystal monolayer adsorbed on it and consequently the alignment of the liquid crystal bulk film.

Acknowledgment. This work was supported by U.S. National Science Foundation Grant DMR-0075402 and partially by Hitachi, Ltd. in Japan. D.K acknowledges the support of KOSEF Grant No. 20004022.

References and Notes

(1) Geary, J. M.; Goodby, J, W,; Kmetz, A. R.; Patel, J. S. *J. Appl. Phys.* **1987**, *62*, 4100.
(2) Zhuang, X.; Marrucci, L.; Shen, Y. R. *Phys. Rev. Lett.* **1994** *73*, 1513.
(3) Sawa. K.; Sumiyoshi, K.; Hirai, Y.; Tateishi, K.; Kamejima, T. *Jpn. J. Appl. Phys.* **1994**, *33*, 6273.
(4) Sakamoto, K.; Arafune, R.; Ito, N.; Ushioda, S.; Suzuki, Y,; Morokawa, S. *J. Appl. Phys.* **1996**, *80*, 431.
(5) Hietpas, G. D.; Sands, J. M.; Allara, D. L. *Macromolecules* **1998**, *31*, 3374.
(6) Seo, D. S.; Araya, K.; Yoshida, N.; Nishikawa, M.; Yabe, Y.; Kobayashi, S. *Jpn. J. Appl. Phys.* **1995**, *34*, L503.
(7) Hirosawa, I. *Jpn. J. Appl. Phys.* **1996**, *35*, 5873.
(8) Kim, Y. B.; Olin, H.; Park, S. Y.; Choi, J. W.; Komitov, L.; Matuszczyk, M.; Lagerwall, S. T. *Appl. Phys. Lett.* **1995**, *66*, 2218.
(9) Kikuchi, H.; Logan, J. A.; Yoon, D. Y. *J. Appl. Phys.* **1996**, *79*, 6811.
(10) Kim, J.-H.; Rosenblatt, C. *J. Appl. Phys.* **2000**, *87*, 155.
(11) Toney, M. F.; Russel, T. P.; Logan, J. A.; Kikuchi, H.; Sands, J. M.; Kumar, S. K. *Nature* **1995**, *374*, 709.
(12) Ouchi, Y.; Mori, I.; Sei. M.; Ito, E.; Araki, T.; Ishii, H.; Seki, K.; Kondo, K. *Physica B* **1995**, *208/209*, 407.
(13) Weiss, K.; Wöll, C.; Böhm, E.; Fiebranz, B.; Forstmann, G.; Peng, B.; Scheumann, V.; Johannsmann, D. *Macromolecules* **1998**, *31*, 1930.
(14) Samant, M. G.; Stöhr, J.; Brown, H. R.; Russel, T. P.; Sand, J. M.; Kumar, S. K. *Macromolecules* **1996**, *29*, 8334.
(15) Stöhr, J.; Samant, M. G.; Cossy-Favre, A.; Diaz, J.; Momoi, Y.; Odahara, S.; Nagata, T. *Macromolecules* **1998**, *31*, 1942.
(16) Zhang, D.; Shen, Y. R.; Somorjai, G. A. *Chem. Phys. Lett.* **1997**, *281*, 394.
(17) Wei, X.; Zhuang, X.; Hong, S.-C.; Goto, T.; Shen, Y. R. *Phys. Rev. Lett.* **1999**, *82*, 4256.
(18) Kim, D.; Shen, Y. R. *Appl. Phys. Lett.* **1999**, *74*, 3314.
(19) Shirota, K.; Yaginuma, M.; Sakai, T.; Ishikawa, K.; Takezoe, H.; Fukuda, A. *Appl. Phys. Lett.* **1996**, *69*, 164.
(20) Meister, R.; Jerome, B. *Macromolecules* **1999**, *32*, 480.
(21) Zhuang, X.; Miranda, P. B.; Kim, D.; Shen, Y. R. *Phys. Rev. B* **1999**, *59*, 12632.
(22) Ishida, H.; Wellinghoff, S. T.; Baer, E.; Koenig, J. L. *Macromolecules* **1980**, *13*, 826.
(23) Wei, X.; Hong, S.-C.; Lvovsky, A. I.; Held, H.; Shen, Y. R. *J. Phys. Chem. B* **2000**, *104*, 3349.
(24) Shen, Y. R. *Appl. Phys. B* **1999**, *68*, 295.

MA0100908